PERGAMON

International Journal of Solids and Structures 37 (2000) 943–958

INTERNATIONAL JOURNAL OF SOLIDS and STRUCTURES

www.elsevier.com/locate/ijsolstr

Three-dimensional Green's functions in anisotropic piezoelectric solids

Ernian Pan*, Fulvio Tonon

Center for Acoustic, Mechanics and Materials, Department of Mechanical Engineering, University of Colorado, Campus Box 427, Boulder, CO 80309-0427, USA

Received 23 December 1998; in revised form 22 March 1999

Abstract

Explicit expressions for three-dimensional extended Green's displacements in general anisotropic piezoelectric solids are derived. A very efficient procedure for the numerical evaluation of the derivatives of the extended Green's displacements is also proposed. Numerical comparisons are carried out for a transversely isotropic piezoelectric solid for which exact closed-form solutions are available. It is found that the extended Green's displacements and their derivatives obtained with the present explicit formulation are in perfect agreement with the exact closed-form solutions. These Green's functions can be used in the boundary integral equations for piezoelectric solids of general anisotropy and for subsequent numerical solutions of these equations by means of the boundary element method.

Keywords: Anisotropy; Piezoelectric solid; 3D Green's function; Radon transform

1. Introduction

Green's functions in three-dimensional (3D) anisotropic media are important to the solution of inclusion problems and of the boundary integral equations. Elastostatic Green's functions in 3D anisotropic media have been studied, for example, by Freedholm (1900), Lifshitz and Rozenzweig (1947), Synge (1957), Willis (1965), Mura and Kinoshita (1971), Pan and Chou (1976). Detailed discussions on the elastic Green's functions in anisotropic solids and their various applications can be found in the review by Bacon et al. (1978) and in the texts of Mura (1987) and Ting (1996). In general, four different methods were previously proposed to calculate the elastostatic Green's functions in 3D anisotropic solids. These are the numerical integral method (Barnett, 1972; Vogel and Rizzo, 1973;

* Corresponding author. Present address: Structures Technology, Inc., 2016 Cameron Street, Suite 213, Raleigh, NC 27605, USA..

E-mail address: pan@ipass.net (E. Pan)

0020-7683/00/$ - see front matter
PII: S0020-7683(99)00073-6

Wilson and Cruse, 1978), series expansion technique (Mura and Kinoshita, 1971; Chang and Chang, 1995; Gray et al., 1996), dual reciprocity technique (Schclar and Partridge, 1993; Perez and Wrobel, 1996), and the eigenvalue/eigenfunction method (Malen, 1971; Deb et al., 1991). While the first three methods are approximate, the last one requires solving a 6×6 eigenvalue problem. Recently, Wang (1997) has obtained explicit expressions for the 3D elastostatic Green's functions in anisotropic materials by use of the Radon transform and contour integration.

Extensive studies have also been carried out on the static Green's functions in anisotropic piezoelectric solids. For both infinite and semi-infinite spaces of transversely isotropic piezoelectric solids, the exact closed-form Green's functions were obtained by Wang and Zheng (1995), Ding et al. (1996), and Dunn and Wienecke (1996, 1998) in terms of potential functions. The exact closed-form Green's functions in two-phase transversely isotropic piezoelectric solids have also been derived recently by Ding et al. (1997). For materials possessing lower elastic and/or electric symmetry, however, the 3D Green's functions were previously evaluated numerically (Deeg, 1980; Chen, 1993; Chen and Lin, 1993), which leads to very cumbersome computation (Chen and Lin, 1995).

In this study, we derive explicit solutions for the extended Green's displacements (three elastic displacements and one electric potential) in a 3D anisotropic piezoelectric solid. In developing the present formulation, we first apply the Radon transform to obtain integral expressions for these Green's displacements. The contour integration involved is then carried out by the residue calculus (Wang, 1997). The derivatives of the extended Green's displacements are evaluated numerically according to a very efficient and robust procedure. Numerical examples are presented for a transversely isotropic piezoelectric solid. It is found that the extended Green's displacements and their derivatives obtained with the present explicit formulation are in perfect agreement with the exact closed-form solutions (Dunn and Wienecke, 1996).

2. Basic equations of linear piezoelectricity

Under the condition of static deformation, a linear and generally anisotropic piezoelectric solid obeys the following governing equations (Tiersten, 1969; Suo et al., 1992; Dunn and Taya, 1993):

2.1. Equilibrium equations

$$\sigma_{ji,\,j} + F_i = 0$$

$$D_{i,\,i} - Q = 0 \tag{1}$$

where σ_{ij} and D_i are the stress and electric displacement, respectively; F_i and Q are the body force and electric charge, respectively. In this and the following sections, summation from 1 to 3 (1–4) over repeated lowercase (uppercase) subscripts is assumed. A subscript comma denotes the partial differentiation.

2.2. Constitutive relations

$$\sigma_{ij} = C_{ijlm}\gamma_{lm} - e_{kij}E_k$$

$$D_i = e_{ijk}\gamma_{jk} + \varepsilon_{ij}E_j \tag{2}$$

where γ_{ij} is the strain and E_i is the electric field; C_{ijlm}, e_{ijk} and ε_{ij} are the elastic moduli (measured at a constant electric field), the piezoelectric coefficients (measured at a constant strain or electric field) and the dielectric constants (measured at a constant strain), respectively. The piezoelectric material constants satisfy the following symmetry relations:

$$C_{ijlm} = C_{jilm} = C_{ijml} = C_{lmij}$$

$$e_{ijk} = e_{ikj}$$

$$\varepsilon_{ij} = \varepsilon_{ji}. \tag{3}$$

It is noteworthy that the elastic and electric fields are generally coupled together. However, uncoupled solutions can be obtained by simply setting $e_{ijk} = 0$.

2.3. Elastic strain-displacement and electric field-potential relations

$$\gamma_{ij} = \frac{1}{2}(u_{i,\,j} + u_{j,\,i})$$

$$E_i = -\phi_{,\,i} \tag{4}$$

where u_i and ϕ are the elastic displacement and electric potential, respectively.

The basic equations presented above can be unified with the notation introduced by Barnett and Lothe (1975). With their notation, the elastic displacement and electric potential, the elastic strain and electric field, the stress and electric displacement, and the elastic and electric moduli can be grouped together as:

$$u_I \begin{cases} u_i & I = 1, 2, 3 \\ \phi & I = 4 \end{cases} \tag{5}$$

$$\gamma_{Ij} = \begin{cases} \gamma_{ij} & I = 1, 2, 3 \\ -E_j & I = 4 \end{cases} \tag{6}$$

$$\sigma_{iJ} = \begin{cases} \sigma_{ij} & J = 1, 2, 3 \\ D_i & J = 4 \end{cases} \tag{7}$$

$$C_{iJKl} = \begin{cases} C_{ijkl} & J, K = 1, 2, 3 \\ e_{lij} & J = 1, 2, 3; K = 4 \\ e_{ikl} & J = 4; K = 1, 2, 3 \\ -\varepsilon_{il} & J, K = 4 \end{cases}. \tag{8}$$

In this and the following sections, the elastic displacement and electric potential, defined by Eq. (5), will be called *extended displacements*, and the elastic stress and electric displacement, defined by Eq. (7), will be called *extended stresses* (Pan, 1999). It is noted that in definitions (5)–(8), the lowercase and uppercase subscripts take on the range 1–3 and 1–4, respectively. Also in these definitions, we have kept

the original symbols instead of introducing new ones since they can be easily distinguished by the range of their subscripts. In terms of this shorthand notation, the constitutive relations can be unified into the single and concise equation:

$$\sigma_{iJ} = C_{iJKl}\gamma_{Kl}. \tag{9}$$

Similarly, the equilibrium equations in terms of the extended stresses can be expressed as

$$\sigma_{iJ,\,i} + F_J = 0 \tag{10}$$

with the extended body force F_J being defined as

$$F_J = \begin{cases} F_j & J = 1,\ 2,\ 3 \\ -Q & J = 4 \end{cases}. \tag{11}$$

3. Integral expressions for Green's displacements

Let $\delta(\mathbf{x}) = \delta(x_1,\ x_2,\ x_3)$ be the Dirac delta function centered at the origin of a space-fixed Cartesian coordinates (O; x_1, x_2, x_3) (Fig. 1(a)) and δ_{JP} the fourth-rank Kronecker delta. The extended Green's displacements (a 4×4 tensor $G_{KP}(\mathbf{x})$) are the fundamental solutions of Eq. (10) caused by an extended point force. Mathematically, this Green's tensor is defined by the partial differential equations:

$$C_{iJKl}G_{KP,\,li}(\mathbf{x}) = -\delta_{JP}\delta(\mathbf{x}). \tag{12}$$

The first index of the Green's tensor denotes the component of the extended displacement, while the second denotes the direction of the extended point force. Since this Green's tensor is generally full for an anisotropic piezoelectric solid, the elastic and electric fields are thus coupled together. That is, a body force will induce an electric potential and an electric charge will generate an elastic displacement. The physical meaning of the extended Green's displacements $G_{KP}(\mathbf{x})$ is: (1) the elastic displacement (K = 1–3) at the field point $\mathbf{x}$ due to a unit force (P = 1–3) at the origin; (2) the elastic displacement (K = 1–3) at the field point $\mathbf{x}$ due to a unit charge (P = 4) at the origin; (3) the electric potential (K = 4) at the field point $\mathbf{x}$ due to a unit force (P = 1–3) at the origin; and finally, (4) the electric potential (K = 4) at the field point $\mathbf{x}$ due to a unit charge (P = 4) at the origin.

To derive the Green's tensor, we need to use the following plane representation of the Dirac delta function (Eq. (A15) of Appendix A)

$$\delta(\mathbf{x}) = -\frac{1}{8\pi^2}\Delta\int_{\Omega}\frac{\delta(\mathbf{n}\cdot\mathbf{x})}{|\ \mathbf{n}\ |^2}\,\mathrm{d}\Omega(\mathbf{n}) \tag{13}$$

where $\mathbf{n}$ is a vector variable with components (n_1, n_2, n_3) in the space-fixed coordinates (O; x_1, x_2, x_3) (Fig. 1(a)), $\Omega(\mathbf{n})$ is any closed surface enclosing the origin (Fig. 1(b)); The integral is taken over all planes defined by $\mathbf{n}\cdot\mathbf{x} = 0$; The dot '$\cdot$' denotes the dot product, and Δ is the 3D Laplacian operator, i.e.

$$\Delta = \frac{\partial^2}{\partial x_1^2} + \frac{\partial^2}{\partial x_2^2} + \frac{\partial^2}{\partial x_3^2}. \tag{14}$$

We now introduce a 4×4 matrix

$$\Gamma_{JK}(\mathbf{n}) = C_{iJKq}n_i n_q \tag{15}$$

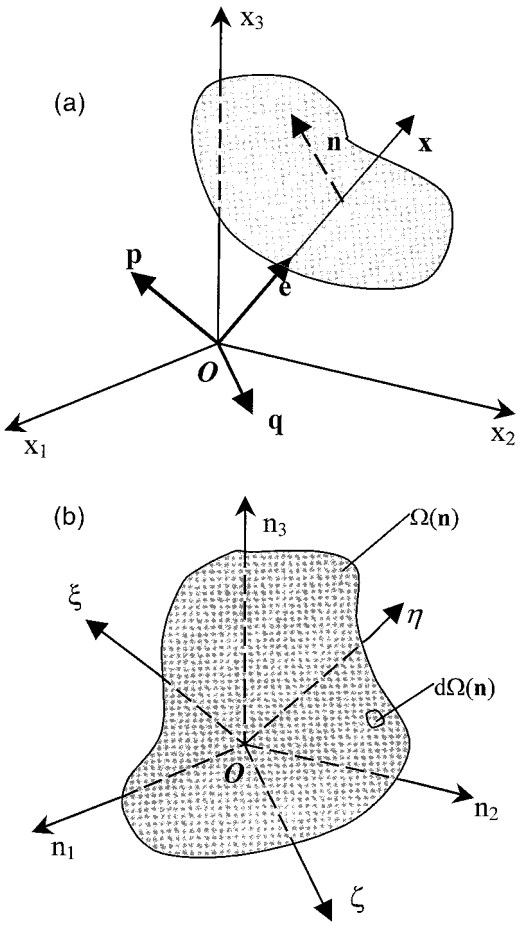

Fig. 1. Relation of the new reference system (O; **e**, **p**, **q**) and the space-fixed Cartesian system (O; x_1, x_2, x_3) in (a), and the geometry of (O; ξ, ζ, η) in the **n**-space in (b).

and denote its inverse by $\Gamma^{-1}_{JK}(\mathbf{n})$. Integrating $\Gamma^{-1}_{JK}(\mathbf{n})\delta(\mathbf{n}\cdot\mathbf{x})$ with respect to **n**, taking its second derivatives with respect to x_i, and multiplying the result by the extended stiffness matrix C_{iJKq}, we then obtain the following important identity (see Eq. (A19) of Appendix A):

$$C_{iJKq}\frac{\partial^2}{\partial x_i \partial x_q}\int_\Omega \Gamma^{-1}_{JK}(\mathbf{n})\delta(\mathbf{n}\cdot\mathbf{x})\,\mathrm{d}\Omega(\mathbf{n}) = \delta_{JP}\Delta\int_\Omega \frac{\delta(\mathbf{n}\cdot\mathbf{x})}{|\,\mathbf{n}\,|^2}\,\mathrm{d}\Omega(\mathbf{n}). \tag{16}$$

Making use of the plane representation (13), Eq. (16) can be rewritten as

$$C_{iJKq}\frac{\partial^2}{\partial x_i \partial x_q}\int_\Omega \Gamma^{-1}_{JK}(\mathbf{n})\delta(\mathbf{n}\cdot\mathbf{x})\,\mathrm{d}\Omega(\mathbf{n}) = -8\pi^2\delta_{JP}\delta(\mathbf{x}). \tag{17}$$

Comparing Eq. (17) to (12), we finally arrive at the following integral expression for the extended Green's displacement tensor

$$G_{JK}(\mathbf{x}) = \frac{1}{8\pi^2}\int_{\Omega} \Gamma^{-1}_{JK}(\mathbf{n})\delta(\mathbf{n}\cdot\mathbf{x})\ \mathrm{d}\Omega(\mathbf{n}) \tag{18}$$

or,

$$G_{JK}(\mathbf{x}) = \frac{1}{8\pi^2}\int_{\Omega} \frac{A_{JK}(\mathbf{n})}{D(\mathbf{n})}\delta(\mathbf{n}\cdot\mathbf{x})\ \mathrm{d}\Omega(\mathbf{n}) \tag{19}$$

where $A_{JK}(\mathbf{n})$ is the adjoint matrix of $\Gamma_{JK}(\mathbf{n})$, while $D(\mathbf{n})$ is the determinant of $\Gamma_{JK}(\mathbf{n})$. These integral expressions for the extended Green's displacement components, similar to those obtained by Deeg (1980) and Chen (1993), are analogous to the anisotropic elastic results (Synge, 1957; Wang, 1997).

4. Explicit expressions for Green's displacements

The integral expression (19) for the Green's tensor can actually be transformed to a 1D infinite integral and the result can then be reduced to a summation of four residues. This is achieved by expressing the vector variable $\mathbf{n}$ in terms of a new, orthogonal, and normalized system (O; $\mathbf{e}$, $\mathbf{p}$, $\mathbf{q}$), instead of the space-fixed Cartesian coordinates (O; x_1, x_2, x_3) (Fig. 1(a) and (b)). In selecting of the new base ($\mathbf{e}$, $\mathbf{p}$, $\mathbf{q}$), we first choose $\mathbf{e}$ as (Wang, 1997)

$$\mathbf{e} = \frac{\mathbf{x}}{r}; \quad r = |\ \mathbf{x}\ |\ . \tag{20}$$

Now, let $\mathbf{v}$ be an arbitrary unit vector different from $\mathbf{e}$ ($\mathbf{v} \neq \mathbf{e}$), the two unit vectors orthogonal to $\mathbf{e}$ can then be selected as:

$$\mathbf{p} = \frac{\mathbf{e}\times\ \mathbf{v}}{|\ \mathbf{e}\times\mathbf{v}\ |}; \quad \mathbf{q} = \mathbf{e}\times\mathbf{p}. \tag{21}$$

It should be emphasized that $\mathbf{e}\times\mathbf{v}$ should be normalized so that $\mathbf{p}$ is a unit vector.

In the new reference system (O; $\mathbf{e}$, $\mathbf{p}$, $\mathbf{q}$), we let the vector variable $\mathbf{n}$ be expressed as

$$\mathbf{n} = \xi\mathbf{p} + \zeta\mathbf{q} + \eta\mathbf{e}. \tag{22}$$

It is clear then that

$$\mathbf{n}\cdot\mathbf{x} = \mathbf{p}\cdot\mathbf{x}\xi + \mathbf{q}\cdot\mathbf{x}\zeta + \mathbf{e}\cdot\mathbf{x}\eta = r\eta. \tag{23}$$

Therefore, in terms of the reference system (O; $\mathbf{e}$, $\mathbf{p}$, $\mathbf{q}$), Eq. (19) becomes

$$G_{JK}(\mathbf{x}) = \frac{1}{8\pi^2}\int_{\Omega} \frac{A_{JK}(\xi\mathbf{p}+\zeta\mathbf{q}+\eta\mathbf{e})}{D(\xi\mathbf{p}+\zeta\mathbf{q}+\eta\mathbf{e})}\delta(r\eta)\ \mathrm{d}\Omega(\xi,\ \zeta,\ \eta) \tag{24}$$

where Ω is again any closed surface enclosing the origin $(\xi,\ \zeta,\ \eta) = (0,\ 0,\ 0)$ (Fig. 1(b)).

The surface integral can be reduced to a 1D infinite integral by following Wang's approach (Wang, 1997). Shown in Fig. 2 is the integral contour composed of a rectangular parallelepiped. This rectangular parallelepiped is bounded by surfaces S_1 and S_2 ($\xi = \pm 1$), S_3 and S_4 ($\zeta = \pm L$), and S_5 and S_6 ($\eta = \pm L$). In terms of these surfaces, the integral (24) can be written as:

$$G_{JK}(\mathbf{x}) = \frac{1}{8\pi^2}\sum_{i=1}^{6}\int_{S_i} \frac{A_{JK}(\xi\mathbf{p}+\zeta\mathbf{q}+\eta\mathbf{e})}{D(\xi\mathbf{p}+\zeta\mathbf{q}+\eta\mathbf{e})}\delta(r\eta)\ \mathrm{d}\Omega(\xi,\ \zeta,\ \eta). \tag{25}$$

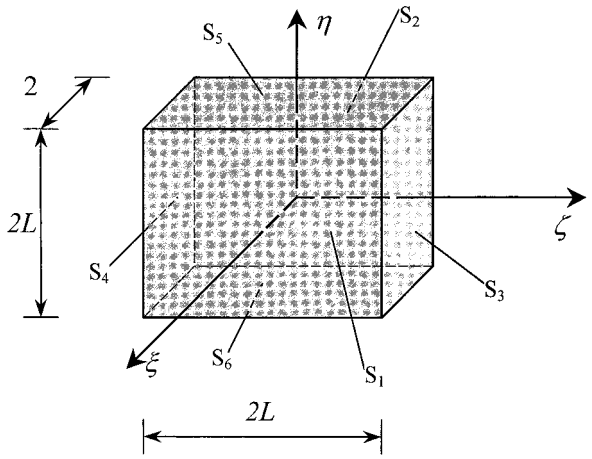

Fig. 2. A rectangular parallelepiped over which the contour integration is carried out. Surfaces S_1 and S_2 are bounded by $\xi = \pm 1$, S_3 and S_4 by $\zeta = \pm L$, and S_5 and S_6 by $\eta = \pm L$.

Since over surfaces other than S_1 and S_2 the integrand in (25) approaches zero as $1/L^2$, their contribution to the integration is zero and Eq. (25) thus becomes

$$G_{JK}(\mathbf{x}) = \frac{1}{8\pi^2}\sum_{i=1}^{2}\int_{S_i}\frac{A_{JK}(\xi\mathbf{p}+\zeta\mathbf{q}+\eta\mathbf{e})}{D(\xi\mathbf{p}+\zeta\mathbf{q}+\eta\mathbf{e})}\delta(r\eta)\,\mathrm{d}\Omega(\xi,\zeta,\eta). \tag{26}$$

We notice that in the integrand of Eq. (26), only even powers of ξ are involved. It is therefore symmetric with respect to ξ. This leads to

$$\begin{aligned} G_{JK}(\mathbf{x}) &= \frac{1}{4\pi^2}\int_{S_l}\frac{A_{JK}(\xi\mathbf{p}+\zeta\mathbf{q}+\eta\mathbf{e})}{D(\xi\mathbf{p}+\zeta\mathbf{q}+\eta\mathbf{e})}\delta(r\eta)\,\mathrm{d}\Omega(\xi,\zeta,\eta) \\ &= \frac{1}{4\pi^2}\int_{-\infty}^{+\infty}\int_{-\infty}^{+\infty}\frac{A_{JK}(\mathbf{p}+\zeta\mathbf{q}+\eta\mathbf{e})}{D(\mathbf{p}+\zeta\mathbf{q}+\eta\mathbf{e})}\delta(r\eta)\,\mathrm{d}\zeta\,\mathrm{d}\eta. \end{aligned} \tag{27}$$

Carrying out the integration of (27) with respect to η yields

$$G_{JK}(\mathbf{x}) = \frac{1}{4\pi^2 r}\int_{-\infty}^{\infty}\frac{A_{JK}(\mathbf{p}+\zeta\mathbf{q})}{D(\mathbf{p}+\zeta\mathbf{q})}\,\mathrm{d}\zeta. \tag{28}$$

Since the inverse of Γ_{JK} exists (Dunn, 1994), its determinant D does not have real roots. Therefore, the eighth-order polynomial equation of ζ

$$D(\mathbf{p}+\zeta\mathbf{q}) = 0 \tag{29}$$

has eight roots, four of them being the conjugate of the remainder. With these roots, we can write the polynomial as

$$D(\mathbf{p}+\zeta\mathbf{q}) = \sum_{k=0}^{8}a_{k+1}\zeta^k = a_9\prod_{m=1}^{4}(\zeta-\zeta_m)(\zeta-\zeta_m^*) \tag{30}$$

where a_9 is the coefficient of ζ^8;

$$\mathrm{Im}\zeta_m > 0; \quad m = 1, 2, 3, 4 \tag{31}$$

and ζ_m^* is the conjugate of ζ_m. Eq. (29) is analogous to the sextic equation of anisotropic elasticity (Head, 1979) and its roots need to be found numerically. These roots can actually be found very efficiently since we are dealing with an eighth-order polynomial with real coefficients (Press et al., 1989).

In terms of the residues at the poles, the extended Green's displacement (28) can be finally expressed explicitly as

$$G_{JK}(\mathbf{x}) = -\frac{\mathrm{Im}}{2\pi r}\sum_{m=1}^{4}\frac{A_{JK}(\mathbf{p}+\zeta_m\mathbf{q})}{a_9(\zeta_m-\zeta_m^*)\prod_{k=1,\ k\neq m}^{4}(\zeta_m-\zeta_k)(\zeta_m-\zeta_k^*)}. \tag{32}$$

There are a couple of features associated with this new expression: First of all, Eq. (32) is an explicit expression. It is therefore very accurate and efficient. For a given pair of field and source points, we need only to solve the 8th-order polynomial Eq. (29) numerically once in order to obtain all the components of the extended Green's displacement and stress (calculation of the extended stress is discussed below). Secondly, in obtaining Eq. (32), we have assumed that all the poles are simple. Should the poles be multiple, a slight change in the material constants will result in single poles, with negligible errors in the computed Green's tensor, as for the purely elastic case (Pan and Amadei, 1996a; Pan, 1997). Thirdly, since Γ_{JK} is symmetric, so is its adjoint A_{JK}. Therefore, the extended Green's displacement G_{JK} is symmetric (Chen, 1993) and one needs to calculate only 10 out of its 16 elements. The symmetric property of the extended Green's tensor can also be considered as a consequence of the Betti-type reciprocity (Pan, 1999). Finally, although one can choose the vector $\mathbf{v}$ ($\neq\mathbf{e}$) arbitrarily, it should be one of the base vectors in the space-fixed Cartesian coordinates, i.e. (1, 0, 0), or (0, 1, 0), or (0, 0, 1). The analytical expression for the extended Green's displacement is much simpler using such a vector $\mathbf{v}$ than using any other vectors.

5. Derivatives of Green's displacements

We have just derived an explicit expression for the extended Green's displacement. In the application of the boundary integral equation, one also needs the extended Green's stress, which can be obtained by taking the derivative of the extended Green's displacement. However, an explicit expression for the derivative of the Green's displacement is too complicated to be implemented efficiently. Although the integral of the derivative of the Green's displacement can be implemented into a boundary element program with some restrictions on the boundary discretization (Wang, 1997), it is desirable to have a direct expression for the derivative of the Green's displacement. Here we propose a numerical evaluation of these derivatives based on the simple Lagrange polynomials. The results turn out to be very efficient and yet very accurate.

Let a function $f(x)$ be known at the n points $x_1 < x_2 < \ldots < x_n$, i.e. $y_i = f(x_i)$ $i = 1, \ldots, n$, and set

$$F(x) = \prod_{k=1}^{n}(x-x_k) \quad F_k(x) = \prod_{r=1,\ r\neq k}^{n}(x-x_r) \quad F_k(x_k) = \prod_{r=1,\ r\neq k}^{n}(x_k-x_r) \tag{33}$$

the Lagrange polynomial of order $n-1$

$$P(x) = \sum_{k=1}^{n}\frac{F_k(x)}{F_k(x_k)}y_k \tag{34}$$

will then interpolate the data, with the complete Lagrange interpolation function being

$$f(x) = P(x) + F(x)\frac{f^{(n)}(\xi(x))}{n!}. \tag{35}$$

If we take the derivative of Eq. (35) and evaluate the result at x_r, we obtain

$$f'(x_r) = P'(x_r) + F'(x_r)\frac{f^{(n)}(\xi(x_r))}{n!}. \tag{36}$$

Thus, the error in the first derivative is

$$F'(x_r)\frac{f^{(n)}(\xi(x_r))}{n!} \tag{37}$$

where $F'(x_r)$ is nothing but the product of the distances between x_r and the other chosen abscissas. If the interval between the chosen abscissas is constant, its minimum value is then attained at the middle point of the segment between x_1 and x_n. Therefore, the best approximation to $f'(x_r)$ obtainable using the polynomial derivative is at the middle point of the segment between x_1 and x_n.

It can be shown that the derivative of the Lagrange polynomial is

$$P'(x_r) = \sum_{k=1,\ k\neq r}^{n} \frac{1}{x_r - x_k}\left[y_r + y_k\frac{F'(x_r)}{F'(x_k)}\right]. \tag{38}$$

If we choose a polynomial of order 2, i.e. with 3 abscissas, we then get

$$f'(x_2) = \frac{1}{2h}[f(x_3) - f(x_1)] - \frac{h^2}{6}f^{(3)}(\xi_2) \tag{39}$$

where $h = x_3 - x_2 = x_2 - x_1$ is the distance between two consecutive abscissas and ξ_2 is a point between x_1 and x_3.

Let $\mathbf{x} = (x_1, x_2, x_3)$ be a field point at which we want to calculate the derivative of the Green's tensor G_{PK} with respect to the coordinates. According to (39), we now have

$$\frac{\partial G_{PK}}{\partial x_1} \approx \frac{1}{2h}[G_{PK}(x_1 + h, x_2, x_3) - G_{PK}(x_1 - h, x_2, x_3)] \tag{40}$$

$$\frac{\partial G_{PK}}{\partial x_2} \approx \frac{1}{2h}[G_{PK}(x_1, x_2 + h, x_3) - G_{PK}(x_1, x_2 - h, x_3)] \tag{41}$$

$$\frac{\partial G_{PK}}{\partial x_3} \approx \frac{1}{2h}[G_{PK}(x_1, x_2, x_3 + h) - G_{PK}(x_1, x_2 x_3 - h)]. \tag{42}$$

The choice of the interval h is a crucial decision. An extensive numerical investigation has led us to the conclusion that the best value of the interval is

$$h = r10^{-6} \tag{43}$$

where r is the distance between the field and source points.

6. Numerical examples

We have been able to implement our formulation into Mathematica. Before doing that, we need to have the elastic tensor C_{ijkl} be expressed in terms of the Voigt constant $c_{\alpha\beta}$, with the latter being defined by

$$\begin{pmatrix} \sigma_{11} \\ \sigma_{22} \\ \sigma_{33} \\ \sigma_{23} \\ \sigma_{13} \\ \sigma_{12} \end{pmatrix} = \begin{pmatrix} c_{11} & c_{12} & c_{13} & c_{14} & c_{15} & c_{16} \\ c_{12} & c_{22} & c_{23} & c_{24} & c_{25} & c_{26} \\ c_{13} & c_{23} & c_{33} & c_{34} & c_{35} & c_{36} \\ c_{14} & c_{24} & c_{34} & c_{44} & c_{45} & c_{46} \\ c_{15} & c_{25} & c_{35} & c_{45} & c_{55} & c_{56} \\ c_{16} & c_{26} & c_{36} & c_{46} & c_{56} & c_{66} \end{pmatrix} \begin{pmatrix} \gamma_{11} \\ \gamma_{22} \\ \gamma_{33} \\ 2\gamma_{23} \\ 2\gamma_{31} \\ 2\gamma_{21} \end{pmatrix} \tag{44}$$

while the relation between C_{ijkl} and $c_{\alpha\beta}$ can be found in Ting (1996).

The piezoelectric constants e_{kij} can also be related to a two-index notation e_{kp} ($k = 1, 2, 3$; $p = 1, \ldots, 6$) in the following way:

$$e_{k1} = e_{k11}; \quad e_{k2} = e_{k22}; \quad e_{k3} = e_{k33}$$

$$e_{k4} = e_{k23} = e_{k32}$$

$$e_{k5} = e_{k12} = e_{k31}$$

$$e_{k6} = e_{k12} = e_{k21}. \tag{45}$$

As a benchmark example, we consider a transversely isotropic piezoelectric material for which an exact closed-form solution is available (Dunn and Wienecke, 1996). Assuming that the axis of the material symmetry is parallel to the x_3-axis, then the non-zero elements of the material constants are:

$$c_{11},\ c_{22}(= c_{11}),\ c_{33},\ c_{13},\ c_{23}(= c_{13}),\ c_{44},\ c_{55}(= c_{44}),\ c_{66},\ c_{12}(= c_{11} - 2c_{66})$$

$$e_{31},\ e_{33},\ e_{15},\ e_{32}(= e_{31}),\ e_{24}(= e_{15})$$

$$\varepsilon_{11},\ \varepsilon_{22}(= \varepsilon_{11}),\ \varepsilon_{33} \tag{46}$$

For a poled lead zirconate titanate (PZT-4) ceramic (Dunn and Taya, 1993), the relevant material constants are given in Table 1, in which the elastic constants $c_{\alpha\beta}$ are in 10^9 N/m^2, the piezoelectric coefficient e_{kp} in C/m^2, and the dielectric constants ε_{ij} in 10^{-9} C/(Vm).

For the source at the origin (0, 0, 0) and the field point at $(x_1, x_2, x_3) = (1, 1, 1)$, the extended Green's displacements and their derivatives are given in Tables 2–5 and are compared to the exact transversely isotropic solution (TI formulation) of Dunn and Wienecke (1996). It is observed that the extended Green's displacements and their derivatives obtained with the present explicit formulation are surprisingly close to the exact closed-form solutions.

7. Conclusions

An explicit expression for the extended Green's displacement in a three-dimensional and general

Table 1
Electroelastic moduli of the PZT-4 material

c_{11}	c_{13}	$c_{12}(=c_{11}-2c_{66})$	c_{33}	c_{44}	c_{66}
139	74.3	77.8	115	25.6	30.6
e_{31}	e_{33}	e_{15}		ε_{11}	ε_{33}
−5.2	15.1	12.7		6.461	5.620

anisotropic piezoelectric solid has been derived. The expression is very easy to implement, robust and efficient, thus allowing the cumbersome numerical evaluation of the extended Green's displacement to be overcome. For the calculation of the derivatives of the extended Green's displacement, we proposed a simple interpolation based on the Lagrange polynomial. As far as the transversely isotropic piezoelectric solid is considered, numerical results of the extended Green's displacements and their derivatives from the present formulation are in perfect agreement with the exact closed-form solutions.

The present formulation is now in the process of being implemented into the authors' 3D boundary element code for purely elastic media (Pan and Amadei, 1996b), which will be accordingly extended to the piezoelectric solid. The corresponding 3D boundary element modeling will be reported in a future paper.

Acknowledgements

The authors are grateful for the support from the National Science Foundation under Grant CMS-9713559 and the Air Force Office of Scientific Research under Grant F49620-98-1-0104. They would also like to thank Professor M. L. Dunn of the Department of Mechanical Engineering, University of Colorado at Boulder, and Dr. C. Y. Wang of Schlumberger for stimulating discussion.

Table 2
Extended Green's displacement G_{PK}

(P, K)	TI formulation	Present formulation	Relative error
1,1	$1.1507372825 \times 10^{-12}$	$1.1507372826 \times 10^{-12}$	1×10^{-10}
1,2	$1.9428530900 \times 10^{-13}$	$1.9428530903 \times 10^{-13}$	1×10^{-10}
1,3	$1.7241444282 \times 10^{-13}$	$1.7241444284 \times 10^{-13}$	1×10^{-10}
1,4	$2.0825816731 \times 10^{-4}$	$2.0825816734 \times 10^{-4}$	1×10^{-10}
2,1	$1.9428530900 \times 10^{-13}$	$1.9428530903 \times 10^{-13}$	1×10^{-10}
2,2	$1.1507372825 \times 10^{-12}$	$1.1507372826 \times 10^{-12}$	1×10^{-10}
2,3	$1.7241444282 \times 10^{-13}$	$1.7241444284 \times 10^{-13}$	1×10^{-10}
2,4	$2.0825816731 \times 10^{-4}$	$2.0825816734 \times 10^{-4}$	1×10^{-10}
3,1	$1.7241444282 \times 10^{-13}$	$1.7241444284 \times 10^{-13}$	1×10^{-10}
3,2	$1.7241444282 \times 10^{-13}$	$1.7241444284 \times 10^{-13}$	1×10^{-10}
3,3	$7.9729216465 \times 10^{-13}$	$7.9729216476 \times 10^{-13}$	1×10^{-10}
3,4	$1.5239325664 \times 10^{-3}$	$1.5239325666 \times 10^{-3}$	1×10^{-10}
4,1	$2.0825816731 \times 10^{-4}$	$2.0825816734 \times 10^{-4}$	1×10^{-10}
4,2	$2.0825816731 \times 10^{-4}$	$2.0825816734 \times 10^{-4}$	1×10^{-10}
4,3	$1.5239325664 \times 10^{-3}$	$1.5239325666 \times 10^{-3}$	1×10^{-10}
4,4	$-4.3915928465 \times 10^{6}$	$-4.3915928471 \times 10^{6}$	1×10^{-10}

Table 3
Derivatives of the extended Green's displacement $G_{PK,1}$

(P, K)	TI formulation	Present formulation	Relative error
1,1	$-9.26183802345 \times 10^{-14}$	$-9.26183801830 \times 10^{-14}$	6×10^{-10}
1,2	$1.65932816546 \times 10^{-14}$	$1.65932813164 \times 10^{-14}$	2×10^{-8}
1,3	$1.82113322728 \times 10^{-14}$	$1.82113326041 \times 10^{-14}$	2×10^{-8}
1,4	$6.70402857710 \times 10^{-6}$	$6.70402926493 \times 10^{-6}$	1×10^{-7}
2,1	$1.65932816546 \times 10^{-14}$	$1.65932813164 \times 10^{-14}$	2×10^{-8}
2,2	$-4.81188998237 \times 10^{-13}$	$-4.81188998226 \times 10^{-13}$	2×10^{-11}
2,3	$-1.54203110547 \times 10^{-13}$	$-1.54203110453 \times 10^{-13}$	6×10^{-10}
2,4	$-2.01554138734 \times 10^{-4}$	$-2.01554137037 \times 10^{-4}$	8×10^{-09}
3,1	$1.82113322728 \times 10^{-14}$	$1.82113326041 \times 10^{-14}$	2×10^{-8}
3,2	$-1.54203110547 \times 10^{-13}$	$-1.54203110453 \times 10^{-13}$	6×10^{-10}
3,3	$-3.30447677887 \times 10^{-13}$	$-3.30447677467 \times 10^{-13}$	1×10^{-9}
3,4	$-6.20021679052 \times 10^{-4}$	$-6.20021678946 \times 10^{-4}$	2×10^{-10}
4,1	$6.70402857711 \times 10^{-6}$	$6.70402926493 \times 10^{-6}$	1×10^{-7}
4,2	$-2.01554138734 \times 10^{-4}$	$-2.01554137037 \times 10^{-4}$	8×10^{-9}
4,3	$-6.20021679052 \times 10^{-4}$	$-6.20021678946 \times 10^{-4}$	2×10^{-10}
4,4	$1.18596300519 \times 10^{6}$	$1.18596296905 \times 10^{6}$	3×10^{-8}

Appendix A

Let $f(\mathbf{x})$ be a function defined in R^3 and s a real number, the *Radon transform* of $f(\mathbf{x})$ is defined as (Courant and Hilbert, 1962; Gel'fand et al., 1966):

$$\hat{f}(s, \mathbf{n}) = R[f(\mathbf{x})] = \int f(\mathbf{x})\delta(s - \mathbf{n} \cdot \mathbf{x})\, d\mathbf{x} \tag{A1}$$

Table 4
Derivatives of the extended Green's displacement $G_{PK,2}$

(P, K)	TI formulation	Present formulation	Relative error
1,1	$-4.81188998237 \times 10^{-13}$	$-4.81188998314 \times 10^{-13}$	2×10^{-10}
1,2	$1.65932816546 \times 10^{-14}$	$1.65932816356 \times 10^{-14}$	1×10^{-9}
1,3	$-1.54203110547 \times 10^{-13}$	$-1.54203110329 \times 10^{-13}$	1×10^{-9}
1,4	$-2.01554138734 \times 10^{-4}$	$-2.01554137136 \times 10^{-4}$	8×10^{-9}
2,1	$1.65932816546 \times 10^{-14}$	$1.65932816356 \times 10^{-14}$	1×10^{-9}
2,2	$-9.26183802345 \times 10^{-14}$	$-9.26183800722 \times 10^{-14}$	2×10^{-9}
2,3	$1.82113322728 \times 10^{-14}$	$1.82113324292 \times 10^{-14}$	9×10^{-9}
2,4	$6.70402857710 \times 10^{-6}$	$6.70402899107 \times 10^{-6}$	6×10^{-8}
3,1	$-1.54203110547 \times 10^{-13}$	$-1.54203110329 \times 10^{-13}$	1×10^{-9}
3,2	$1.82113322728 \times 10^{-14}$	$1.82113324292 \times 10^{-14}$	9×10^{-9}
3,3	$-3.30447677887 \times 10^{-13}$	$-3.30447678318 \times 10^{-13}$	1×10^{-9}
3,4	$-6.20021679052 \times 10^{-4}$	$-6.20021678915 \times 10^{-4}$	2×10^{-10}
4,1	$-2.01554138734 \times 10^{-4}$	$-2.01554137136 \times 10^{-4}$	8×10^{-9}
4,2	$6.70402857711 \times 10^{-6}$	$6.70402899107 \times 10^{-6}$	6×10^{-8}
4,3	$-6.20021679052 \times 10^{-4}$	$-6.20021678915 \times 10^{-4}$	2×10^{-10}
4,4	$1.18596300519 \times 10^{6}$	$1.18596303172 \times 10^{6}$	2×10^{-8}

Table 5
Derivatives of the extended Green's displacement $G_{PK,3}$

(P, K)	TI formulation	Present formulation	Relative error
1,1	$-5.76929903985 \times 10^{-13}$	$-5.76929904374 \times 10^{-13}$	7×10^{-10}
1,2	$-2.27471872311 \times 10^{-13}$	$-2.27471872962 \times 10^{-13}$	3×10^{-9}
1,3	$-3.64226645455 \times 10^{-14}$	$-3.64226646215 \times 10^{-14}$	2×10^{-9}
1,4	$-1.34080571542 \times 10^{-5}$	$-1.34080565033 \times 10^{-5}$	5×10^{-8}
2,1	$-2.27471872311 \times 10^{-13}$	$-2.27471872962 \times 10^{-13}$	3×10^{-9}
2,2	$-5.76929903985 \times 10^{-13}$	$-5.76929904047 \times 10^{-13}$	1×10^{-10}
2,3	$-3.64226645455 \times 10^{-14}$	$-3.64226648904 \times 10^{-14}$	9×10^{-9}
2,4	$-1.34080571542 \times 10^{-5}$	$-1.34080580158 \times 10^{-5}$	6×10^{-8}
3,1	$-3.64226645455 \times 10^{-14}$	$-3.64226646215 \times 10^{-14}$	2×10^{-9}
3,2	$-3.64226645455 \times 10^{-14}$	$-3.64226648904 \times 10^{-14}$	9×10^{-9}
3,3	$-1.36396808876 \times 10^{-13}$	$-1.36396808802 \times 10^{-13}$	5×10^{-10}
3,4	$-2.83889208291 \times 10^{-4}$	$-2.83889208747 \times 10^{-4}$	2×10^{-9}
4,1	$-1.34080571542 \times 10^{-5}$	$-1.34080565033 \times 10^{-5}$	5×10^{-8}
4,2	$-1.34080571542 \times 10^{-5}$	$-1.34080580158 \times 10^{-5}$	6×10^{-8}
4,3	$-2.83889208291 \times 10^{-4}$	$-2.83889208747 \times 10^{-4}$	2×10^{-9}
4,4	$2.01966683615 \times 10^{6}$	$2.01966682620 \times 10^{6}$	5×10^{-9}

where $\delta(\ )$ is the one-dimensional Dirac delta. It follows that, when s varies over the real line, the Radon transform is an integration of $f(\mathbf{x})$ over all planes defined by $\mathbf{n} \cdot \mathbf{x} = s$.

From definition (A1), we can get the following properties of $\hat{f}$:

1. Homogeneity:

$$\hat{f}(\alpha s, \alpha \mathbf{n}) = \frac{\hat{f}(s, \mathbf{n})}{|\alpha|}. \tag{A2}$$

2. Linearity:

$$R[c_1 f_1 + c_2 f_2] = c_1 \hat{f}_1 + c_2 \hat{f}_2. \tag{A3}$$

3. Transform of a linear transformation:

$$R[f(\mathbf{A}^{-1}\mathbf{x})] = |\ \det\ \mathbf{A}\ |\, \hat{f}(s, \mathbf{A}^{\mathrm{T}}\mathbf{n}) \tag{A4}$$

where $\det \mathbf{A} \neq 0$.

4. Transform of derivatives:

$$R\left[\frac{\partial f}{\partial x_i}\right] = n_i \frac{\partial \hat{f}(s, \mathbf{n})}{\partial s}; \quad R\left[\frac{\partial^2 f}{\partial x_i \partial x_j}\right] = n_i n_j \frac{\partial^2 \hat{f}(s, \mathbf{n})}{\partial s^2}. \tag{A5a,b}$$

The *inverse Radon transform* is an integration in the $\mathbf{n}$-space over the surface Ω containing the origin, defined as:

$$f(\mathbf{x}) = R^*(\hat{f}'') = -\frac{1}{8\pi^2}\int_{\Omega} \hat{f}''(\mathbf{n} \cdot \mathbf{x}, \mathbf{n})\ \mathrm{d}\Omega(\mathbf{n}) \tag{A6}$$

where

$$\hat{f}''(\mathbf{n}\cdot\mathbf{x},\,\mathbf{n}) = \left.\frac{\partial^2 \hat{f}(s,\,\mathbf{n})}{\partial s^2}\right|_{s=\mathbf{n}\cdot\mathbf{x}}. \tag{A7}$$

Let $\delta(\mathbf{x}) = \delta(x_1,\, x_2,\, x_3)$ be the three-dimensional Dirac delta centered at the origin, i.e.

$$\int_{R^3} \delta(\mathbf{x}) f(\mathbf{x})\, \mathrm{d}V = f(\mathbf{o}) \tag{A8}$$

then, the Radon transform of the three-dimensional Dirac delta is

$$\hat{\delta}(s,\,\mathbf{n}) = R[\delta(\mathbf{x})] = \int \delta(\mathbf{x})\delta(s-\mathbf{n}\cdot\mathbf{x})\, \mathrm{d}\mathbf{x} = \delta(s-\mathbf{n}\cdot\mathbf{o}) = \delta(s). \tag{A9}$$

In Eq. (A8), $\mathbf{o} = (0,\, 0,\, 0)$. We will use the same symbol δ for one-dimensional as well as three-dimensional Dirac delta, with the convention that if its argument is a scalar, the one-dimensional Dirac delta is involved; if the argument is a vector, the three-dimensional Dirac delta is involved.

Noticing

$$\frac{\partial \delta(\mathbf{n}\cdot\mathbf{x})}{\partial x_i} = n_i \left.\frac{\mathrm{d}\delta}{\mathrm{d}s}\right|_{s=\mathbf{n}\cdot\mathbf{x}}; \quad \frac{\partial^2 \delta(\mathbf{n}\cdot\mathbf{x})}{\partial x_i^2} = n_i^2 \left.\frac{\mathrm{d}^2\delta}{\mathrm{d}s^2}\right|_{s=\mathbf{n}\cdot\mathbf{x}} \tag{A10}$$

we obtain

$$\sum_{i=1}^{3} \frac{\partial^2 \delta(\mathbf{n}\cdot\mathbf{x})}{\partial x_i^2} = \sum_{i=1}^{3} n_i^2 \left.\frac{\mathrm{d}^2\delta}{\mathrm{d}s^2}\right|_{s=\mathbf{n}\cdot\mathbf{x}} = \left.\frac{\mathrm{d}^2\delta}{\mathrm{d}s^2}\right|_{s=\mathbf{n}\cdot\mathbf{x}} \sum_{i=1}^{3} n_i^2 = |\,\mathbf{n}\,|^2 \left.\frac{\mathrm{d}^2\delta}{\mathrm{d}s^2}\right|_{s=\mathbf{n}\cdot\mathbf{x}}. \tag{A11}$$

In terms of the 3D Laplacian operator, Eq. (A11) can be rewritten as

$$\frac{\Delta\delta(\mathbf{n}\cdot\mathbf{x})}{|\,\mathbf{n}\,|^2} = \left.\frac{\mathrm{d}^2\delta}{\mathrm{d}s^2}\right|_{s=\mathbf{n}\cdot\mathbf{x}}. \tag{A12}$$

Therefore, Eq. (A7) becomes

$$\hat{\delta}''\left.\frac{\mathrm{d}^2\delta}{\mathrm{d}s^2}\right|_{s=\mathbf{n}\cdot\mathbf{x}} = \frac{\Delta\delta(\mathbf{n}\cdot\mathbf{x})}{|\,\mathbf{n}\,|^2}. \tag{A13}$$

According to (A6), the inverse Radon transform of the Dirac delta is

$$\delta(\mathbf{x}) = -\frac{1}{8\pi^2}\int_{\Omega} \frac{\Delta\delta(\mathbf{n}\cdot\mathbf{x})}{|\,\mathbf{n}\,|^2}\, \mathrm{d}\Omega(\mathbf{n}) = -\frac{1}{8\pi^2}\Delta\int_{\Omega} \frac{\delta(\mathbf{n}\cdot\mathbf{x})}{|\,\mathbf{n}\,|^2}\, \mathrm{d}\Omega(\mathbf{n}). \tag{A14}$$

The last equal sign is due to the fact that the variable of integration is $\mathbf{n}$, not $\mathbf{x}$. Thus, we finally arrive at the very notable plane representation of $\delta(\mathbf{x})$:

$$\delta(\mathbf{x}) = -\frac{1}{8\pi^2}\Delta\int_{\Omega} \frac{\delta(\mathbf{n}\cdot\mathbf{x})}{|\,\mathbf{n}\,|^2}\, \mathrm{d}\Omega(\mathbf{n}). \tag{A15}$$

Furthermore, from Eq. (A3) and (A5b), we get

$$R[\Delta f(\mathbf{x})] = \sum_{i=1}^{3} R\left[\frac{\partial^2 f(\mathbf{x})}{\partial x_i^2}\right] = \sum_{i=1}^{3} n_i^2 \frac{\partial^2 \hat{f}(s,\,\mathbf{n})}{\partial s^2} = \frac{\partial^2 \hat{f}(s,\,\mathbf{n})}{\partial s^2} \sum_{i=1}^{3} n_i^2 = |\,\mathbf{n}\,|^2 \frac{\partial^2 \hat{f}(s,\,\mathbf{n})}{\partial s^2}. \tag{A16}$$

Making use of Eq. (A10), we now can derive the following identities, in which integration is taken over the **n**-space:

$$C_{iJKq}\frac{\partial^2}{\partial x_i \partial x_q}\int_\Omega \Gamma^{-1}_{JK}(\mathbf{n})\delta(\mathbf{n}\cdot\mathbf{x})\,\mathrm{d}\Omega = C_{iJKq}\int_\Omega \Gamma^{-1}_{pk}(\mathbf{n})\frac{\partial^2\delta(\mathbf{n}\cdot\mathbf{x})}{\partial x_i \partial x_q}\,\mathrm{d}\Omega$$

$$= C_{iJKq}\int_\Omega \Gamma^{-1}_{pk}(\mathbf{n})n_i n_q \frac{\mathrm{d}^2\delta(s)}{\mathrm{d}s^2}\bigg|_{s=\mathbf{n}\cdot\mathbf{x}}\mathrm{d}\Omega = \int_\Omega C_{iJKq}n_i n_q \Gamma^{-1}_{pk}(\mathbf{n})\frac{\mathrm{d}^2\delta(s)}{\mathrm{d}s^2}\bigg|_{s=\mathbf{n}\cdot\mathbf{x}}\mathrm{d}\Omega$$

$$= \int_\Omega C_{iJKq}n_i n_q (C_{iJKq}n_i n_q)^{-1}\frac{\mathrm{d}^2\delta(s)}{\mathrm{d}s^2}\bigg|_{s=\mathbf{n}\cdot\mathbf{x}}\mathrm{d}\Omega = \delta_{JP}\int_\Omega \frac{\mathrm{d}^2\delta(s)}{\mathrm{d}s}\bigg|_{s=\mathbf{n}\cdot\mathbf{x}}\mathrm{d}\Omega. \tag{A17}$$

By virtue of (A13), we have

$$\delta_{JP}\int_\Omega \frac{\mathrm{d}^2\delta(s)}{\mathrm{d}s^2}\bigg|_{s=\mathbf{n}\cdot\mathbf{x}}\mathrm{d}\Omega = \delta_{JP}\int_\Omega \frac{\Delta\delta(\mathbf{n}\cdot\mathbf{x})}{|\,\mathbf{n}\,|^2}\,\mathrm{d}\Omega = \delta_{JP}\Delta\int_\Omega \frac{\delta(\mathbf{n}\cdot\mathbf{x})}{|\,\mathbf{n}\,|^2}\,\mathrm{d}\Omega. \tag{A18}$$

Summing up, we obtain the following important identity:

$$C_{iJKq}\frac{\partial^2}{\partial x_i \partial x_q}\int_\Omega \Gamma^{-1}_{JK}(\mathbf{n})\delta(\mathbf{n}\cdot\mathbf{x})\,\mathrm{d}\Omega = \delta_{JP}\Delta\int_\Omega \frac{\delta(\mathbf{n}\cdot\mathbf{x})}{|\,\mathbf{n}\,|^2}\,\mathrm{d}\Omega. \tag{A19}$$

It is worth mentioning that the Radon transform, as well as the direct delta function method, were also successfully applied to the derivation of the elastodynamic Green's functions for anisotropic solids (Wang and Achenbach, 1995; Tewary, 1995).

References

Bacon, D.J., Barnett, D.M., Scattergood, R.O., 1978. The anisotropic continuum theory of lattice defects. Progress in Materials Sci. 23, 51–262.

Barnett, D.M., 1972. The precise evaluation of derivatives of the anisotropic elastic Green's functions. Physica Status Solidi 49b, 741–748.

Barnett, D.M., Lothe, J., 1975. Dislocation and line charges in anisotropic piezoelectric insulators. Physica Status Solidi 67b, 105–111.

Chang, C.S., Chang, Y., 1995. Green's function for elastic medium with general anisotropy. Journal of Applied Mechanics 62, 573–578.

Chen, T., 1993. Green's functions and the non-uniform transformation problem in a piezoelectric medium. Mech. Res. Comm. 20, 271–278.

Chen, T., Lin, F.Z., 1993. Numerical evaluation of derivatives of the anisotropic piezoelectric Green's functions. Mech. Res. Comm. 20, 501–506.

Chen, T., Lin, F.Z., 1995. Boundary integral formulations for three-dimensional anisotropic piezoelectric solids. Computational Mechanics 15, 485–496.

Courant, R., Hilbert, D., 1962. Methods of Mathematical Physics, vol. II. Interscience, New York.

Deb, A., Henry Jr, D.P., Wilson, R.B., 1991. Alternate BEM formulations for 2- and 3-D anisotropic thermoelasticity. International Journal of Solids and Structures 27, 1721–1738.

Deeg, W.F. 1980 The analysis of dislocation, crack, and inclusion problems in piezoelectric solids. Ph.D. dissertation, Stanford University.

Ding, H., Chen, B., Liang, J., 1996. General solutions for coupled equations for piezoelectric media. International Journal of Solids Structures 33, 2283–2298.

Ding, H., Chen, B., Liang, J., 1997. On the Green's functions for two-phase transversely isotropic piezoelectric media. International Journal of Solids Structures 34, 3041–3057.

Dunn, M.L., 1994. Electroelastic Green's functions for transversely isotropic piezoelectric media and their application to the solution of inclusion and inhomogeneity problems. Int. J. of Eng. Sci. 32, 119–131.
Dunn, M.L., Taya, M., 1993. An analysis of piezoelectric composite materials containing ellipsoidal inhomogeneities. Proc. R. Soc. Lond. A443, 265–287.
Dunn, M.L., Wienecke, H.A., 1996. Green's functions for transversely isotropic piezoelectric solids. International Journal of Solids Structures 33, 4571–4581.
Dunn, M.L., Wienecke, H.A. 1999 Half-space Green's functions for transversely isotropic piezoelectric solids. J. Appl. Mech. (in press).
Freedholm, I., 1900. Sur les equations de l'equilibre d'un corps solide elastique. Acta Mathematica 23, 1–42.
Gel'fand, I.M., Graev, M.I., Vilenkin, Y.N., 1966. Generalized Functions, vol. 5. Academic Press, New York.
Gray, L.J., Ghosh, D., Kaplan, T., 1996. Evaluation of the anisotropic Green's functions in three dimensional elasticity. Computational Mechanics 17, 255–261.
Head, A.K., 1979. The Gaois unsolvability of the sextic equation of anisotropic elasticity. Journal of Elasticity 9, 9–20.
Lifshitz, I.M., Rozenzweig, L.N., 1947. On the construction of the Green's tensor for the basic equation of the theory of elasticity of an anisotropic infinite medium. Zh. Eksp. Teor. Fiz. 17, 783–791.
Malen, K., 1971. A unified six-dimensional treatment of elastic Green's functions and dislocations. Physica Status Solidi 44b, 661–672.
Mura, T., 1987. Micromechanics of Defects in Solids, 2nd ed. Martinus Nijhoff.
Mura, T., Kinoshita, N., 1971. Green's functions for anisotropic elasticity. Physica Status Solidi 47b, 607–618.
Pan, E., 1997. A general boundary element analysis of 2-D linear elastic fracture mechanics. Int. J. Fracture 88, 41–59.
Pan, E., 1999. A BEM analysis of fracture mechanics in 2-D anisotropic piezoelectric solids. Eng. Anal. Bound. Elements 23, 67–76.
Pan, E., Amadei, B., 1996a. Fracture mechanics analysis of cracked 2-D anisotropic media with a new formulation of the boundary element method. Int. J. Fracture 77, 161–174.
Pan, E., Amadei, B., 1996b. 3-D boundary element formulation of anisotropic elasticity with gravity. Applied Mathematical Modelling 20, 114–120.
Pan, Y.C., Chou, T.W., 1976. Point force solution for an infinite transversely isotropic solid. Journal of Applied Mechanics 43, 608–612.
Perez, M.M., Wrobel, L.C., 1996. An integral-equation formulation for anisotropic elastostatics. Journal of Applied Mechanics 63, 891–902.
Press, W.H., Flannery, B.P., Teukolsky, S.A., Vetterling, W.T., 1989. Numerical Recipes. Cambridge University Press.
Schclar, N.A., Partridge, P.W., 1993. 3D anisotropic elasticity with BEM using the isotropic fundamental solution. Engineering Analysis with Boundary Elements 11, 137–144.
Suo, Z., Kuo, C.M., Barnett, D.M., Willis, J.R., 1992. Fracture mechanics for piezoelectric ceramics. J. Mech. Phys. Solids 40, 739–765.
Synge, J.L., 1957. The Hypercircle in Mathematical Physics. Cambridge University Press.
Tewary, V.K., 1995. Computationally efficient representation for elastostatic and elastodynamic Green's functions for anisotropic solids. Physical Review B51, 15,695–15,702.
Tiersten, H.F., 1969. Linear Piezoelectric Plate Vibrations. Plenum Press, New York.
Ting, T.C.T., 1996. Anisotropic Elasticity—Theory and Applications. Oxford University Press, New York.
Vogel, S.M., Rizzo, F.J., 1973. An integral equation formulation of three dimensional anisotropic elastostatic boundary value problems. Journal of Elasticity 3, 203–216.
Wang, C.Y., 1997. Elastostatic fields produced by a point source in solids of general anisotropy. J. Eng. Math. 32, 41–52.
Wang, C.Y., Achenbach, J.D., 1995. Three-dimensional time-harmonic elastodynamic Green's functions for anisotropic solids. Proc. R. Soc. Lond. A449, 441–458.
Wang, Z., Zheng, B., 1995. The general solution of three-dimensional problems in piezoelectric media. International Journal of Solids Structures 32, 105–115.
Willis, J.R., 1965. The elastic interaction energy of dislocation loops in anisotropic media. Q. J. Mech. Appl. Math. 18, 419–433.
Wilson, R.B., Cruse, T.A., 1978. Efficient implementation of anisotropic three dimensional boundary-integral equation stress analysis. International Journal for Numerical Methods in Engineering 12, 1383–1397.